Ireri A. Sustaita-Torres, Sergio Haro-Rodríguez and Rafael Colás*

Aging of a Low Carbon Heat Resistant Cast Alloy

DOI 10.1515/htmp-2016-0112
Received June 13, 2016; accepted December 30, 2016

Abstract: The changes in microstructure that take place during aging a low carbon heat resistant alloy at 750°C for a period of time of up to 1,000 h were studied by optical and scanning electron microscopy, X-ray diffraction and mechanical testing. The microstructure of the as-cast alloy consisted of an austenitic matrix and a network of Nb- and Cr-rich primary carbides that were identified by their tonality when viewed in backscattered mode in a scanning electron microscopy. Aging promotes precipitation of secondary carbides and the transformation of the Nb-rich particles. The mechanical properties are affected by the occurrence of the different phenomena.

Keywords: heat-resisting cast alloys, precipitation, aging, microstructural evolution

Introduction

Heat-resistant alloys are used in environments subjected to oxidizing or corrosive atmospheres at temperatures above 650 °C. Their main constituents are nickel, chromium and iron, and contain different amounts of niobium, titanium, vanadium and zirconium to enhance their creep resistance by the formation of particles stable at the operating temperatures. Their chemical compositions have changed through their use during the last 50 years; early alloys were cast conventional stainless steels (HB and HC types, 18Cr-4Ni and 18Cr-8Ni), that turned into HK (25Cr-20Ni) and HP (25Cr-35Ni) types. The purpose for the reduction in fuel consumption and in emissions impose harsher operating conditions in many industrial sectors, and so the new heat resistant alloys contain reduced amounts of carbon and higher amounts of chromium and nickel, as well as and many other elements [1–12].

***Corresponding author: Rafael Colás,** Facultad de Ingeniería Mecánica y Eléctrica, Universidad Autónoma de Nuevo León, Nicolás de los Garza, México, E-mail: rafael.colas@uanl.edu.mx
Ireri A. Sustaita-Torres: E-mail: ireri.sustaita@gmail.com, **Sergio Haro-Rodríguez:** E-mail: haros@uaz.edu.mx, Unidad Académica de Ingeniería, Universidad Autónoma de Zacatecas, 98000 Zacatecas, México

Experimental procedure

Samples from a heat resistant alloy (0.15 C, 16.8 Fe, 34.0 Cr, 1.53 Si, 1.31 Nb, 1.03 Mn, 0.08 P, 0.02 P, 0.01 S, bal. Ni, mass %) were cut from a centrifugal cast pipe of 1500 mm in length with internal and external diameters of 108 and 130 mm, respectively; cylindrical tensile specimens of 25 mm in length and 6.4 mm in diameter were machined with their axis parallel to that of the pipe. The tests were conducted at room temperature in material that was either in their as-cast and or aged conditions; Vickers microhardness tests (200 g for 15 s) were also conducted. The material was held at 750 °C for up to 1000 h in air in an electric resistance furnace. The samples were prepared for their metallographic examination following standard polishing procedures and were etched with an electrolytic solution of 10 g of oxalic acid in 100 ml of water. A potential of 6 V was applied for 3–5 s using a stainless steel cathode; the temperature of the etchant was kept at 26 °C.

The microstructure of specimens in the as-cast conditions and aged for 500 and 1000 h were examined in an inverted light optical microscope (LOM). A scanning electron microscope (SEM) was used to evaluate the microstructure of selected samples using secondary (SE) and backscattered electron (BE) detectors. X-ray analyses of selected areas were also obtained (EDX). The presence of different phases was identified by X-ray diffraction (XRD) using copper radiation ($\lambda = 0.15418$ nm) in the interval of 2θ of 20 to 100° with a time step 13 s and 2 θ of 0.02°.

Results and discussion

Optical examination of the as-cast samples shows that the microstructure of the alloy is made of an austenite dendrite matrix, with a secondary dendrite arm spacing of 40 μm, and a network of primary eutectic carbides present in the interdendritic regions (Figure 1). Figure 2 shows images taken from the alloy using the detector for SE, Figure 2(a), and BE, Figure 2(b). The difference in tonality of the carbides can be appreciated, as heavier elements appear in lighter tones. Selected EDX analyses carried out on the matrix and on either type of carbide show that the bright particles contain niobium, whereas

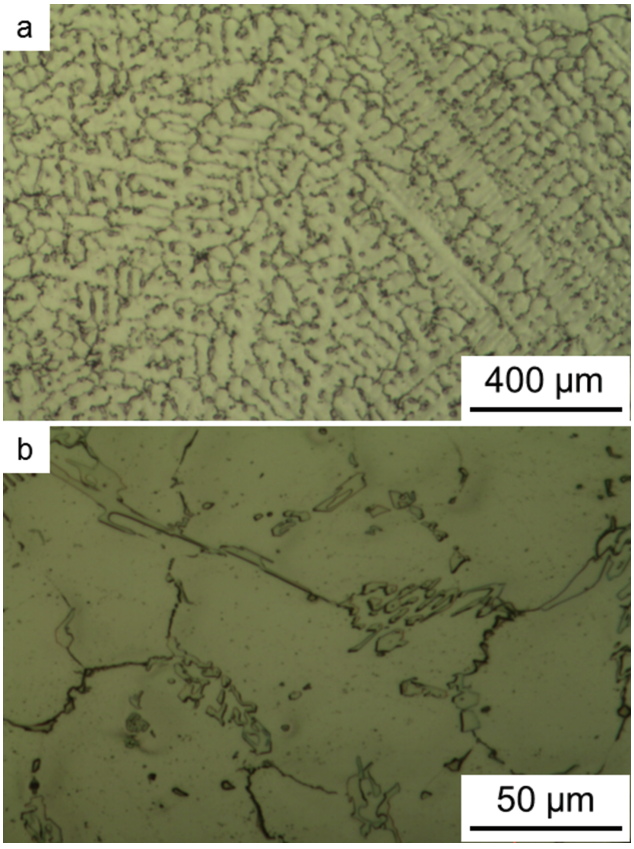

Figure 1: Light optical micrographs of the as-cast alloy at two magnifications.

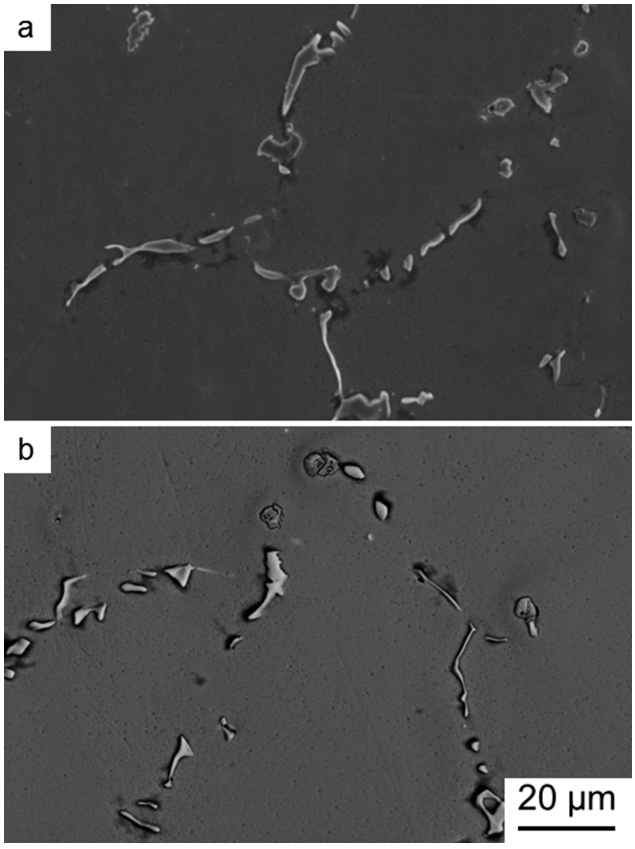

Figure 2: Scanning electron micrographs of the as-cast alloy using secondary (a) and backscattered (b) electron detectors.

the dark carbides are rich in chromium (Figure 3), in agreement with work published before [8–11].

Aging promote changes in the microstructure of the alloy. Figure 4 shows the SEM images, in BE mode, of the material after aging for 500 and 1000 h. The most remarkable features in the aged samples are the precipitation of small secondary needle-shape particles and the rounding of primary carbides, as compared with the as-cast microstructures shown in Figure 2. Figures 5 and 6 show selected EDX analyses conducted in the dark and light particles in as-cast and aged samples. Selected EDX analyses were carried out on the secondary carbides found in the aged alloys; such results are shown in Figure 7 that indicate that these particles are made of chromium; the presence of Ni and Si in the spectra may be due to the small size of the particles so their signal may come from surrounding matrix. The X-ray spectra obtained in the samples in the as-cast and aged conditions are shown in Figure 8.

Figure 4 shows that secondary carbides have the tendency to grow along well defined directions, as the angles between different needle-shape were inclined either 60 or 90° to each other, indicating that the particles align to <110> directions (it can be deduced by crystallographic means that any two different [110] directions are inclined either 60 or 90° with respect to each other) [12]. As planes and directions normal to each other have the same index in the cubic system, it can be deduced that the growing particles are $Cr_{23}C_6$, as these carbides nucleate and grow on {110} planes [13]. The FCC lattice parameter for the $Cr_{23}C_6$ carbides was calculated from the XRD diffraction charts yielding to 1.075 nm, which is consistent with the values of 1.06 to 1.11 nm reported in the literature [14–16].

Chromium and niobium form different carbides that are stable at different temperatures [17–20]. The experimental data obtained by X-ray diffraction, Figure 8, indicate that the primary eutectic carbides are of the NbC and Cr_7C_3. Aging promotes the occurrence of secondary $Cr_{23}C_6$ and that of a silicide identified as Nb_3Ni_2Si. Research carried out on similar alloys have shown NbC transforms to a silicide referred as

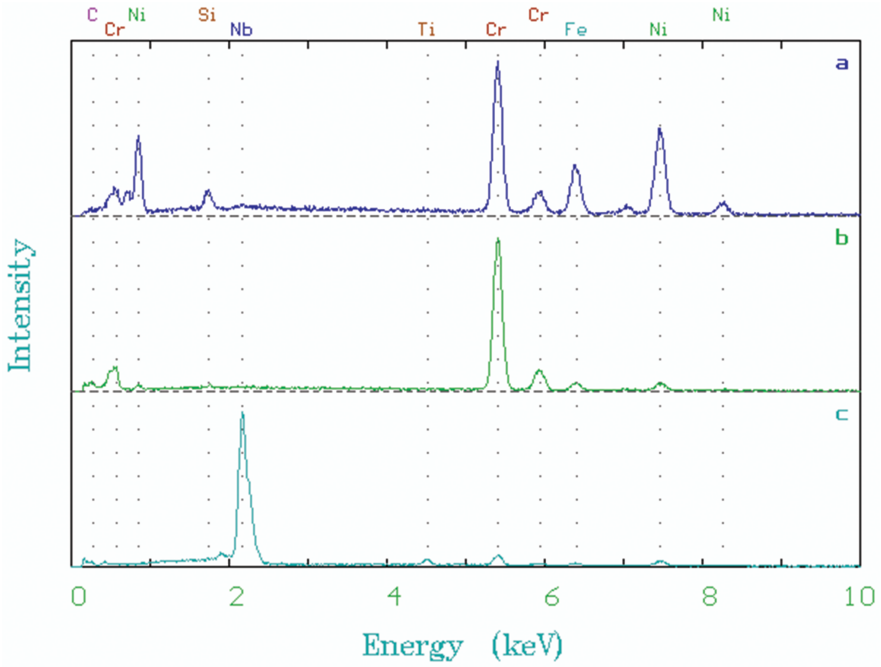

Figure 3: EDX spectra of selected area analyses of the matrix (a) and the dark (b) and light carbides (c) in the as-cast alloy.

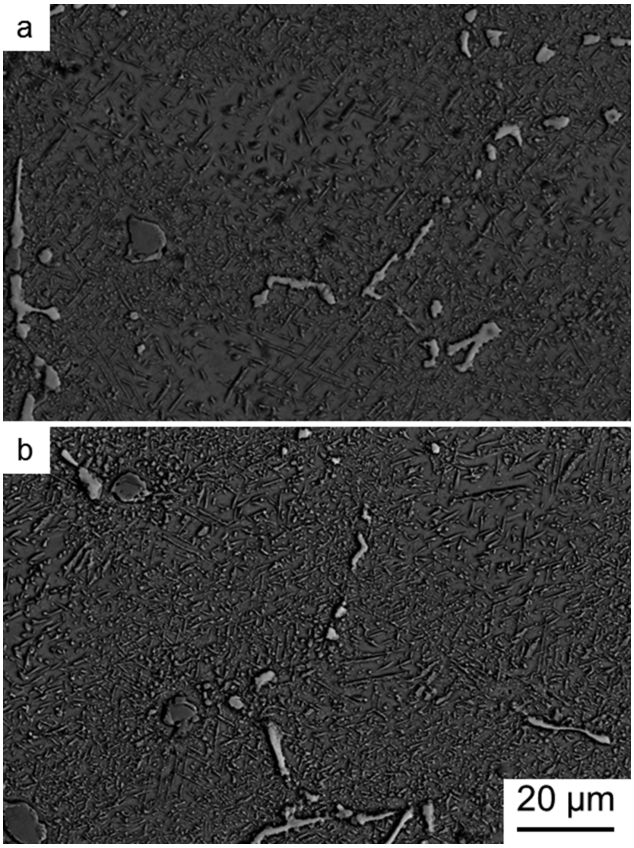

Figure 4: BE detector scanning electron micrographs of alloy aged for 500 (a) and 1000 h (b).

either η- or G-phase [6, 11, 15, 21–24]. Figure 9 shows a SEM image in backscattered electron mode of a sample aged for 1000 h in which partial transformation of niobium-rich carbide into silicide takes place, confirming that this transformation takes place by diffusion [24], and is not complete even after 1000 h of aging. It has been suggested that carbon is released during this process, producing a local increase in solute that promotes the precipitation of $Cr_{23}C_6$ [21]. The Nb_3Ni_2Si structure that was identified in the XRD charts in the aged condition has a FCC structure with a lattice parameter of 1.12 nm, which agrees with results from previous researchers [6, 11, 15, 21–24]. Further details on this transformation can be found elsewhere [11].

The changes that take place during aging affect the mechanical properties of the material, promoting the reduction in ductility and the increase in strength and hardness, Table 1. The values obtained in this work coincide with those from similar alloys [1, 9, 11, 14] (Figure 10). The reduction in ductility becomes critical when these alloys have to be repaired by welding after service, as the low value of ductility will not allow the repair without an adequate annealing heat treatment [10, 25]; these materials are sensitive to weld cracking, as cracks are formed in the brittle zones created by primary carbides [26]. It is claimed that η-phase acts as nucleation point of weld cracks in aged samples that are able to grow through

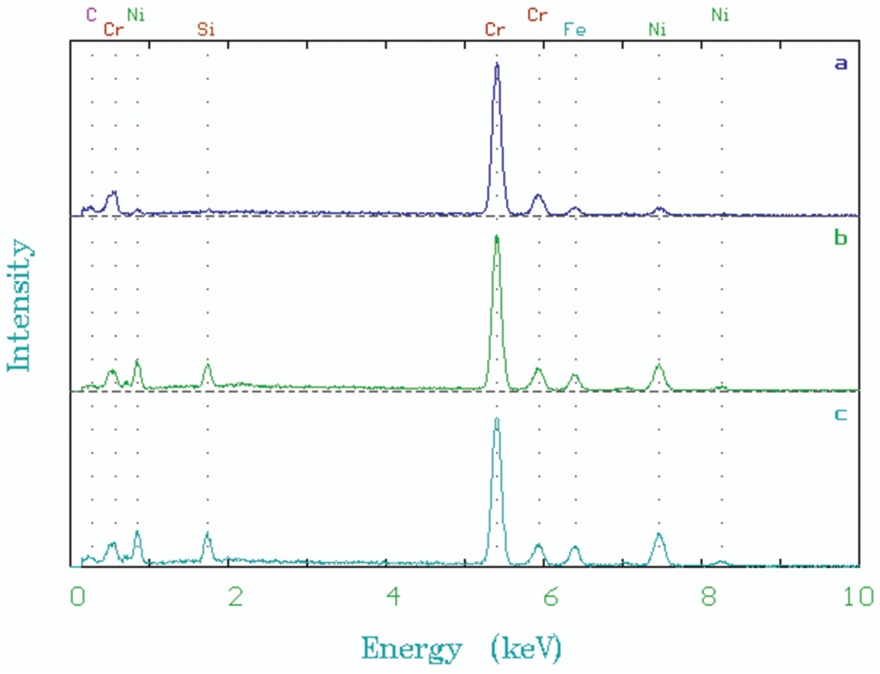

Figure 5: EDX spectra of selected area analyses of the chromium rich carbides in the as-cast (a) and aged for 500 (b) and 1000 h (c).

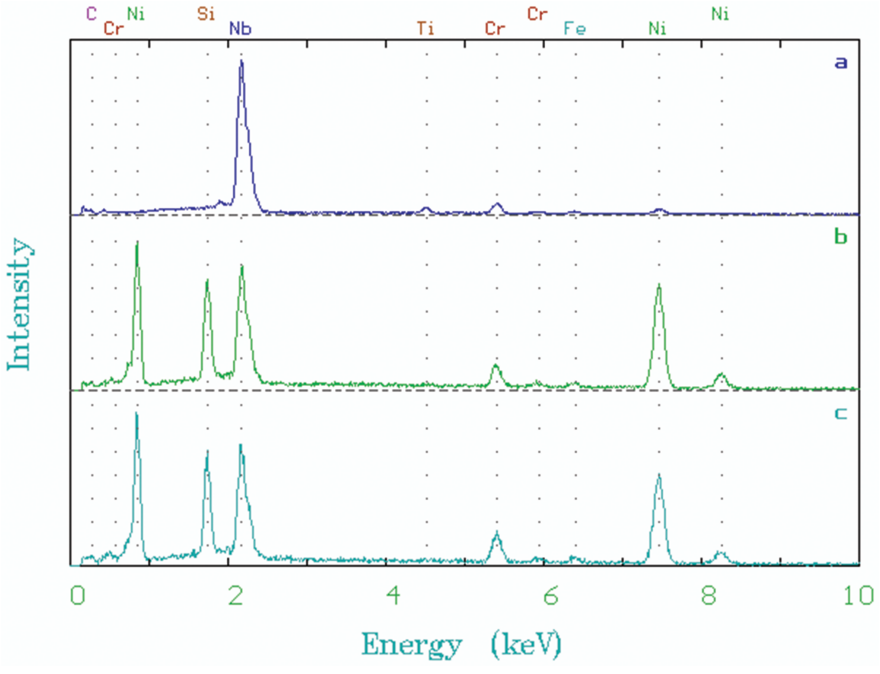

Figure 6: EDX spectra of selected area analyses of the niobium rich carbides in the as-cast (a) and aged for 500 (b) and 1000 h (c).

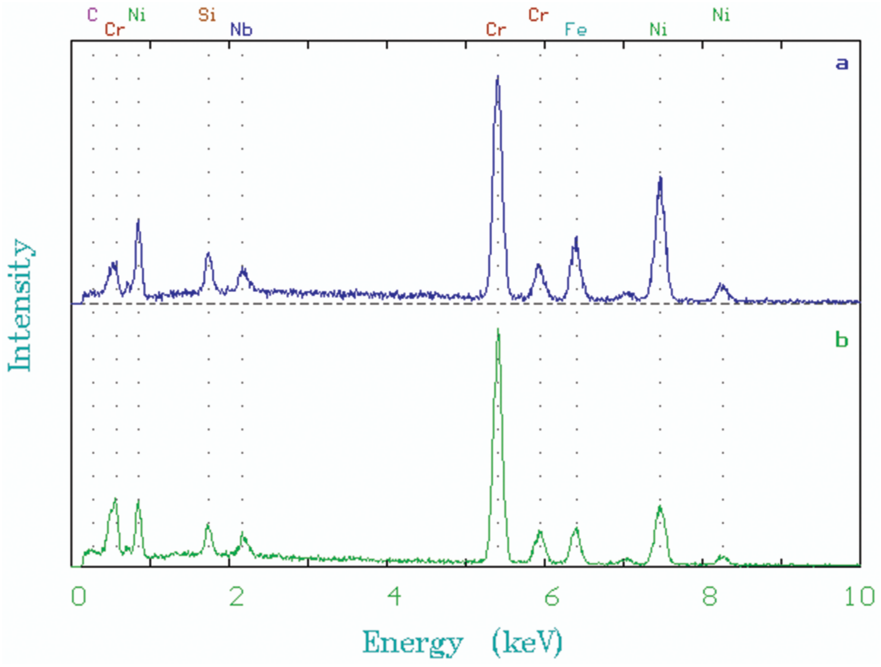

Figure 7: EDX spectra of the secondary precipitates in samples aged for 500 (a) and 1000 h (b).

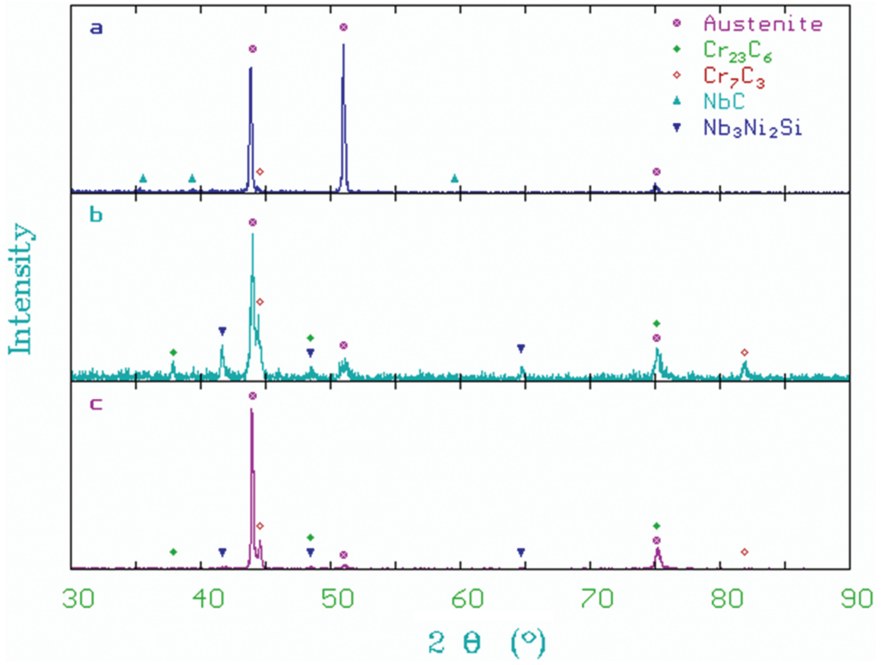

Figure 8: X-ray diffraction spectra in the as-cast (a) and aged for 500 (b) and 1000 h (c).

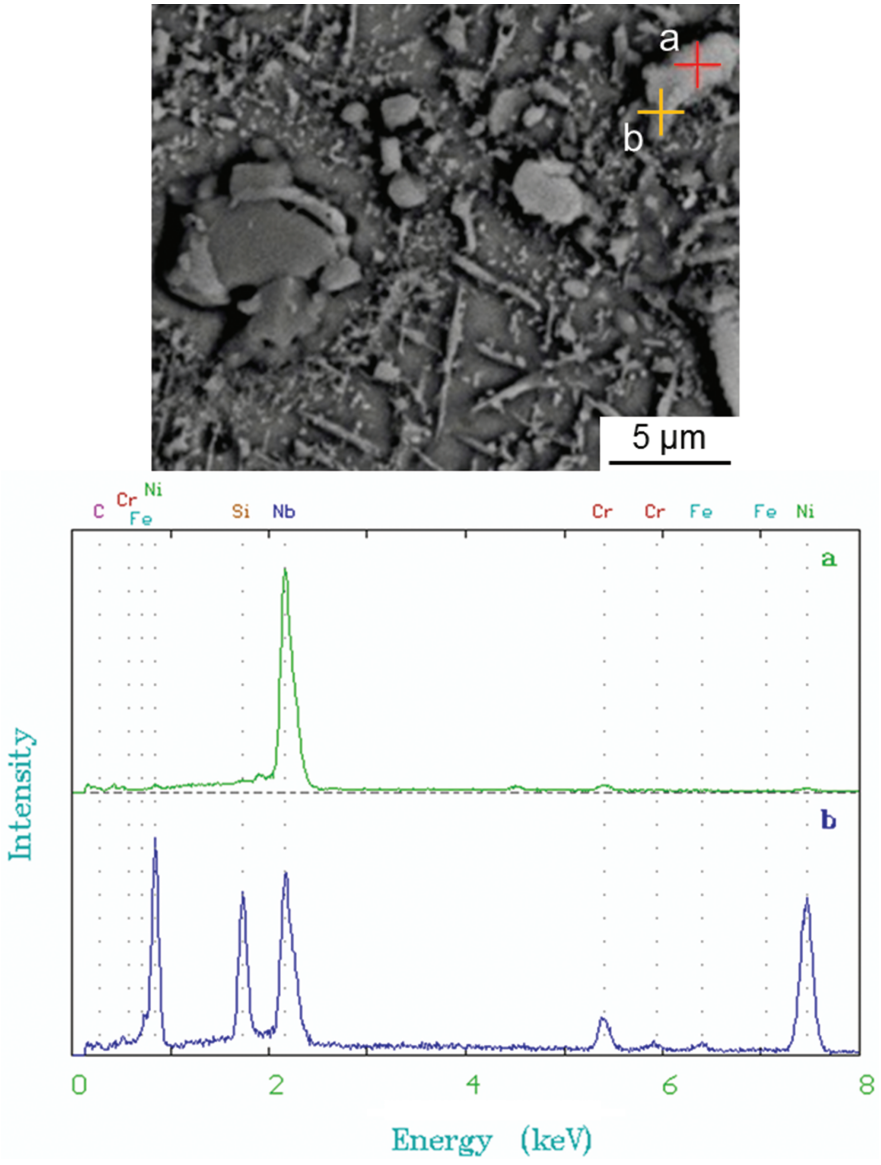

Figure 9: SEM image in backscattered electron mode of a sample from the low-carbon alloy aged for 1000 h showing the partial transformation of a NbC (a) particle into the niobium silicide (b). The EDX spectra are shown at the bottom.

$M_{23}C_6$ carbides [22]. The interface between matrix and G-phase has been identified as preferential site for nucleation of cracks due to creep [23, 24].

Table 1: Mechanical properties at room temperature.

Condition	Tensile strength (MPa)	Elongation (%)	Hardness (HVN)
As-cast	337	5.63	174
Aged 500 h	447	1.75	266
Aged 1000 h	441	0.81	286

Conclusions

It can be summarized that the microstructure of the as-cast material is made of an austenitic dendrite matrix and a network of primary carbides present in interdendritic areas. The scanning electron microscopy image in back-scattered electrons mode revealed that the carbides are of two different types. EDX microanalysis showed that niobium-rich carbides appear bright, whereas chromium-rich appear in darker tones. XRD analyses revealed the presence of NbC and Cr_7C_3 in the as-cast condition. Aging for different time at 750°C produced changes in the

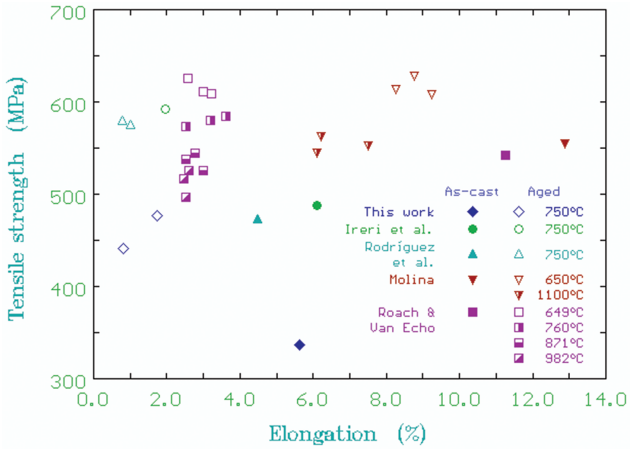

Figure 10: Changes in the tensile strength and ductility due to aging. Data from the literature are added for comparison [1, 9, 11, 14].

morphology and chemical composition of the primary phases and the precipitation of secondary $Cr_{23}C_6$ carbides. It was found that NbC transforms by diffusion into Nb_3Ni_2Si. Aging affects the mechanical properties of the material, as hardness and tensile strength increase, but ductility is reduced.

Acknowledgments: The authors thank the support from the Mexican National Council for Science and Technology (CONACYT) and the Program for the Improvement of Professorship (PRODEP) from the Ministry for Public Education (SEP) Mexico.

Funding: Consejo Nacional de Ciencia y Tecnolog.

References

[1] D.B. Roach and J.A. Van Echo, Stainless steel castings, ASTM STP 756, Philadelphia (1982), pp. 275–312.
[2] W.T. Hou and R.W.K. Honeycombe, Mater. Sci. Technol., 1 (1985) 385–389.
[3] W.T. Hou and R.W.K. Honeycombe, Mater. Sci. Technol., 1 (1985) 390–397.
[4] S.J. Zhu, J. Zhao and F.G. Wang, Metal. Trans. A, 21A (1990) 2237–2241.
[5] C.W. Thomas, M. Borshevsky and A.N. Marshall, Mater. Sci. Technol., 8 (1992) 855–861.
[6] G.D. Barbabela, L.H. Almeida, T.L. Silveira and I. Le May, Mater. Charact., 26 (1991) 193–197.
[7] G.D.A. Soares, L.H. Almeida, T.L. Silveira and I. Le May, Mater. Charact., 29 (1992) 387–396.
[8] J. Rodríguez, S. Haro, A. Velasco and R. Colás, Mater. Charact., 45 (2000) 25–32.
[9] J. Rodríguez, S. Haro, A. Velasco and R. Colás, Int. J. Cast Met. Res., 17 (2004) 188–192.
[10] S. Haro, D. López, A. Velasco and R. Viramontes, Mater. Chem. Phys., 66 (2000) 90–96.
[11] I.A. Sustaita-Torres, S. Haro-Rodríguez, M.P. Guerrero-Mata, M. de la Garza, E. Valdés, F. Deschaux-Beaume and R. Colás, Mater. Chem. Phys., 133 (2012) 1018–1023.
[12] H.K.D.H. Bhadeshia, Worked Examples in the Geometry of Crystals, 2nd, The Institute of Metals, London (2006).
[13] J.W. Martin, Micromechanisms in Particle-Hardened Alloys, Cambridge University Press, Cambridge (1980).
[14] J.O. Molina, PhD Thesis, Facultad de Ingeniería Mecánica y Eléctrica, Universidad Autónoma de Nuevo León, México (1992).
[15] J. Laigo, F. Christien, R.L. Gall, F. Tancret and J. Furtado, Mater. Charact., 59 (2008) 1580–1586.
[16] H. Kimura and Y. Sasaki, Trans. Jpn. Inst. Met., 2 (1961) 98–104.
[17] S.R. Shatynski, Oxid. Met., 13 (1979) 105–118.
[18] M. Venkatraman and J.P. Neumann, Bull. Alloy Phase Diagrams, 11 (1990) 152–159.
[19] Y. He, Z. Li, H. Qi and W. Gao, Mat. Res. Innovations, 1 (1997) 157–160.
[20] K. Shinozaki, H. Kuroki, Y. Nakao, K. Nishimoto, M. Inui and M. Takahashi, Welding Int., 13 (1999) 39–48.
[21] D.J. Powell, R. Pilkington and D.A. Miller, Acta. Metall., 36 (1988) 713–724.
[22] L.H. de Almeida, P.R.O. Emygdio, I. Le May and F.C. Ferraz, Key to Advances in Materials, Vol. 24 edited by M.G. Burke, E.A. Clark and E.J. Palmiere, American Society for Metals, Materials Park (1996), pp. 193–198.
[23] B. Piekarski, Mater. Charact., 47 (2001) 181–186.
[24] L.H. de Almeida, A.F. Ribeiro and I. Le May, Mater. Charact., 49 (2002) 219–229.
[25] H.W. Ebert, Welding J., 55 (1976) 939–945.
[26] A. Duchosal, F. Deschaux-Beaume, C. Bordreuil, G. Fras and P. Lours, Sci. Techn. Welding Joining, 13 (2008) 126–135.
[27] R.A.P. Ibañez, G.D.A. Soares, L.H. Almeida and I. Le May, Mater. Charact., 30 (1993) 243–249.